Cell

KIF4 Motor Regulates Activity-Dependent Neuronal Survival by Suppressing PARP-1 Enzymatic Activity

Ryosuke Midorikawa,[1] Yosuke Takei,[1] and Nobutaka Hirokawa[1,*]
[1] Department of Cell Biology and Anatomy, Graduate School of Medicine, University of Tokyo, Hongo 7-3-1, Bunkyo-ku, Tokyo 113-0033, Japan
*Contact: hirokawa@m.u-tokyo.ac.jp
DOI 10.1016/j.cell.2006.02.039

SUMMARY

In brain development, apoptosis is a physiological process that controls the final numbers of neurons. Here, we report that the activity-dependent prevention of apoptosis in juvenile neurons is regulated by kinesin superfamily protein 4 (KIF4), a microtubule-based molecular motor. The C-terminal domain of KIF4 is a module that suppresses the activity of poly (ADP-ribose) polymerase-1 (PARP-1), a nuclear enzyme known to maintain cell homeostasis by repairing DNA and serving as a transcriptional regulator. When neurons are stimulated by membrane depolarization, calcium signaling mediated by CaMKII induces dissociation of KIF4 from PARP-1, resulting in upregulation of PARP-1 activity, which supports neuron survival. After dissociation from PARP-1, KIF4 enters into the cytoplasm from the nucleus and moves to the distal part of neurites in a microtubule-dependent manner. We suggested that KIF4 controls the activity-dependent survival of postmitotic neurons by regulating PARP-1 activity in brain development.

INTRODUCTION

The kinesin superfamily (KIF) of proteins are microtubule-based motor proteins specialized in the transport of membrane organelles, protein complexes, and mRNAs (Hirokawa, 1998; Hirokawa and Takemura, 2005). Kinesin superfamily protein 4 (KIF4), a KIF member classified in Kinesin-4 in the standardized nomenclature (Lawrence et al., 2004), is strongly expressed in juvenile tissues including differentiated young neurons, where it localizes in nuclei and growth cones (Aizawa et al., 1992; Sekine et al., 1994). In growth cones, KIF4 colocalizes with membranous organelles, suggesting its role in vesicle transport (Sekine et al., 1994; Peretti et al., 2000). On the other hand, several possible KIF4 homologs have been identified: chromokinesin (chicken; Wang and Adler, 1995), XKLP1 (*Xenopus*; Vernos et al., 1995), and hKIF4A (human; Oh et al., 2000; Lee et al., 2001). These homologs are reported to be mitotic motors implicated in chromosome segregation during mitosis. Thus, the physiological function of KIF4 is controversial and its role in postmitotic neurons remains obscure.

Here, we demonstrate that KIF4 regulates programmed cell death of juvenile neurons by interacting directly with poly (ADP-ribose) polymerase-1 (PARP-1), a nuclear enzyme that modifies various nuclear proteins with poly ADP-ribosylation (Althaus and Richter, 1987; D'Amours et al., 1999). When activated by DNA damage or biological signals, PARP-1 maintains cell homeostasis through repairing DNA, controlling the energy balance, and serving as a transcriptional regulator (Griesenbeck et al., 1999; Tulin and Spradling, 2003). It is reported that in fetal neurons, membrane depolarization induces activation of PARP-1 via Ca^{2+} influx into nucleoplasm (Homburg et al., 2000). Our results demonstrated that PARP-1 activation prevents neuronal apoptosis, which is regulated by KIF4 in a manner dependent on membrane depolarization. We suggest that the control of PARP-1 activity by KIF4 underlies the activity-dependent neuronal survival that contributes to the organization of the nervous system via regulating the number of neurons during brain development.

RESULTS

Mitotic Division Is Normal in Cells Lacking KIF4

Using a gene-targeting strategy, we generated ES cell clones with disrupted *kif4* genes as a tool for investigating the function of KIF4 (see Figure S1 in the Supplemental Data available with this article online). Because *kif4* gene is located on sex chromosome X, single homologous recombination at the *kif4* locus is enough to generate *kif4* null ($kif4^{-/Y}$) ES cell clones. Three independent *kif4* null ($kif4^{-/Y}$) clones (1, 2, and 3) were used throughout the study. $Kif4^{-/Y}$ cells did not show any difference in the shape or size of colonies, compared with wild-type ($kif4^{+/Y}$) cells (Figure S2A). To examine the role of KIF4 in

mitosis, we performed DNA analysis of these cells using flow cytometry. There was no difference between genotypes in the distributions of the DNA contents of the cells (Figure S2B), suggesting that chromosome segregation and mitotic cell division were intact in the *kif4*$^{-/Y}$ cells.

KIF4 Binds Directly to PARP-1

The nonmotor domain of KIF4 (the tail domain—amino acids no.1005–1231) is expected to associate with a specific binding protein (Nakagawa et al., 2000). To identify proteins binding to KIF4 in 5-day-old mouse brain, the tail domain of KIF4 fused to GST was prepared as bait for screening (GST-KIF4 tail in Figure 1Aa). After incubation of brain homogenates with GST-KIF4 tail beads, the 110 kDa band was specifically eluted with 1.0 M NaCl buffer (Figure 1Ab, arrow), not only with the GST beads (Figure 1Ac). In this condition, this was the only band identified as a possible binding partner for KIF4. Amino acid sequencing and mass spectrometry revealed that the 110 kDa protein was PARP-1 (data not shown).

KIF4 and PARP-1 were coimmunoprecipitated from cell lysates using either anti-KIF4 or anti-PARP-1 antibodies, but not from lysates of *kif4*$^{-/Y}$ cells (Figure 1B). Furthermore, purified recombinant GST-KIF4 tail was demonstrated to bind to purified PARP-1 (Figure 1C). In this experiment, about half of the PARP-1 in the reaction buffer was collected from GST-KIF4 tail beads, whereas no complex formation was detected from control beads (Figure 1C). Next, to exclude the possibility that KIF4 and PARP-1 form a complex through their binding to DNA, we compared in vitro complex formation between in the presence and absence of DNA. DNA did not affect complex formation (Figure 1C), and DNA pull-down assays also revealed that the KIF4 tail domain did not bind to DNA, whereas PARP-1 did, as previously reported (Figure 1D). Collectively, we conclude that KIF4 binds to PARP-1 by direct interaction.

KIF4 Suppresses Enzymatic Activity of PARP-1

To examine the possible effect of KIF4 on PARP-1 enzymatic activity, we analyzed in vitro automodification of PARP-1 with poly (ADP-ribose) (PAR). ^{32}P-NAD labeling represents the auto-poly ADP-ribosylation of PARP-1 (Figure 2A). The addition of the KIF4 tail domain inhibited automodification in a dose-dependent manner (Figure 2A), indicating that the binding of the KIF4 tail domain suppresses PARP-1 activity. Next, to examine the in vivo interaction of KIF4 with PARP-1, we transfected various KIF4-GFP constructs into NIH 3T3 cells (Figure 2B). Full length and headless KIF4-GFP colocalized with native PARP-1 in the nucleus (Figure 2Bb). However, tailless KIF4-GFP, which lacks a PARP-1 binding site, localized not only in the nucleus but also in cytoplasm (Figure 2Bb). These results suggest that the nuclear localization of KIF4 is mediated by its binding to PARP-1. Next, to examine functional aspects of the KIF4-PARP-1 interaction, PARP-1 activation induced by H_2O_2 treatment was compared among cells transfected with the constructs.

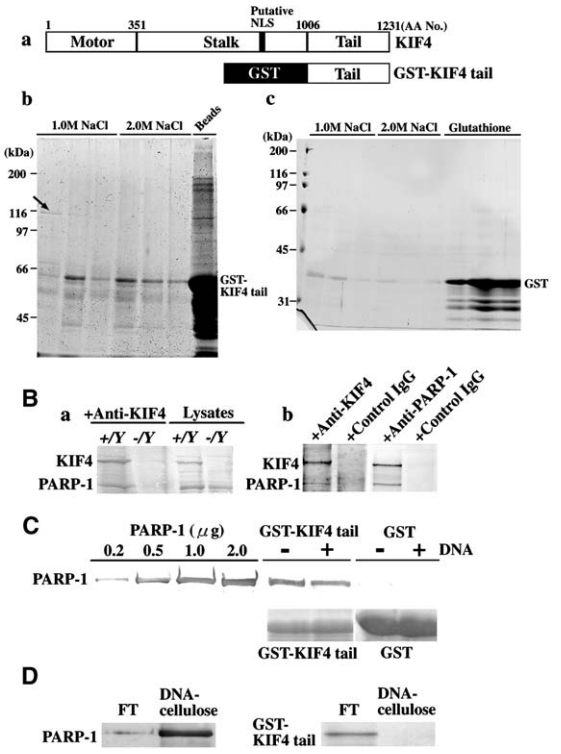

Figure 1. KIF4 Binds to PARP-1 with Its Tail Domain

(A) Screening of KIF4 binding protein. (a) Structural view of full length KIF4 and GST-KIF4 tail fusion proteins. Putative NLS (nuclear localization signal, amino acids no. 794–799; Lee et al., 2001) is depicted. (b) GST pull-down. P110 in 1.0 M NaCl-eluents are visualized by Coomassie brilliant blue (arrow). Each lane corresponds to sequential elution (three times in 1.0 M NaCl buffer and three times in 2.0 M NaCl buffer, respectively). (c) Negative control using only GST.

(B) Immunoprecipitation of ES cell lysates (a) and fibroblast cell lysates (b) show that KIF4 and PARP-1 form a complex. Immunoblotting of lysates is also presented in (a). IgG was used for negative control experiments in (b).

(C) In vitro binding assay. About a half of the PARP-1 is collected by the GST-KIF4 tail beads. Various amounts of PARP-1 were loaded in the left four lanes for a comparison. The presence of DNA did not affect the results.

(D) DNA pull-down using DNA-cellulose. PARP-1 binds to DNA but GST-KIF4 tail does not. FT: flow through.

PARP-1 activity was quantified by measuring the fluorescence intensity of anti-PAR antibody (10H) labeling. Cells expressed with full-length and headless KIF4-GFP that contain the PARP-1 binding (tail) domain of KIF4 showed lower immunoreactivity, whereas the expression of tailless KIF4-GFP that lacks PARP-1 binding domain did not have such an effect, suggesting that tail domain is the responsible region in KIF4 to suppress PARP-1 activity in vivo (Figures 2Bc and 2Bd). Biochemical measurement of the PARP-1 activities of lysates of the transfected cells also confirmed the suppression of PARP-1 activity by the overexpression of the full-length and headless KIF4-GFP constructs (Figure 2Be). Treatment with 3-aminobenzamide (3-AB), a PARP inhibitor, blocked upregulation of PARP-1

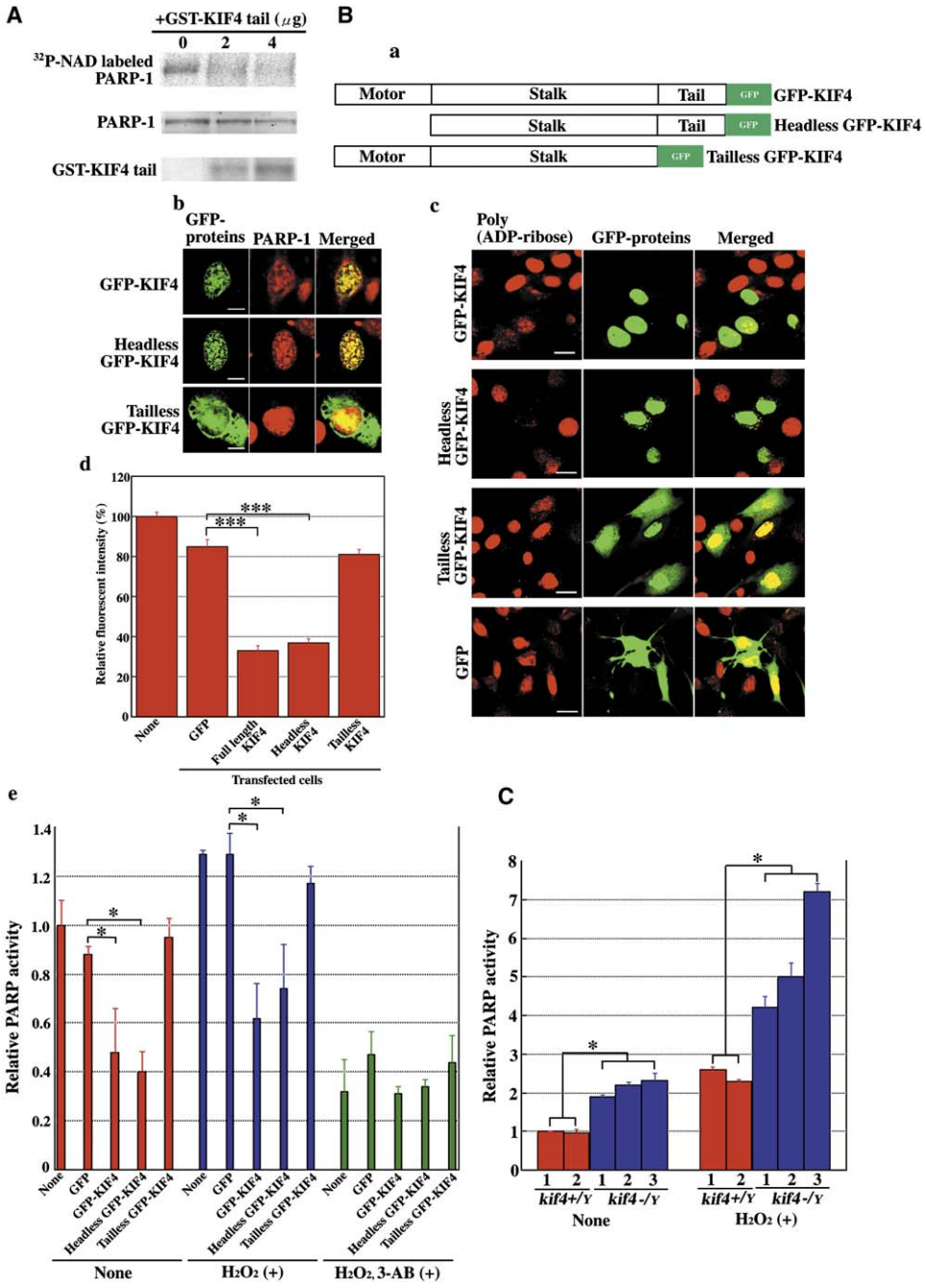

Figure 2. Regulation of PARP-1 Enzymatic Activity by KIF4

(A) Effect of KIF4 tail on PARP-1 automodification. ^{32}P-NAD-labeled PARP-1 represents the automodification of PARP-1, which is inhibited by the addition of GST-KIF4 tail (upper panel). Activated calf-thymus DNA (Scovassi et al., 1984) was added to each sample. Immunoblotting using anti-PARP-1 and anti-GST antibodies is shown in the middle and lower panels.

(B) Overexpression of deletion mutants. (a) Structure of GFP-fusion proteins. (b) Fluorescent images of transfected cells. Bar = 10 μm. (c) Immunolabeling of transfected cells with anti-poly (ADP-ribose) (PAR) antibody after PARP-1 activation by DNA damage. Bar = 10 μm. (d) Measurement of fluorescence intensities using anti-PAR antibody. A total of 300 transfected cells in three independent experiments were examined. Mean ± SEM is presented (***$p < 0.001$; t test). (e) Biochemical measurement of PARP-1 activity of lysates of transfected cells. The transfection efficiency of each vector was adjusted to about 35%. Each value was calculated from three independent experiments. Mean ± SD is presented (*$p < 0.05$; t test).

(C) PARP-1 activity of *kif4*$^{+/Y}$ and *kif4*$^{-/Y}$ ES cells before and after PARP-1 activation by H_2O_2-induced DNA damage. Three independent *kif4*$^{-/Y}$ ES cell clones were analyzed. Data were collected from five experiments. Mean ± SEM is presented (*$p < 0.05$; t test).

activity induced by H_2O_2 treatment, irrespective of the presence or absence of the transfected constructs (Figure 2Be). Consistently, PARP-1 activity was upregulated in *kif4*$^{-/Y}$ ES cells both with and without H_2O_2 treatment (Figure 2C). Taken together, we conclude that KIF4 suppresses PARP-1 activity through the binding of its tail domain with PARP-1.

Neurons Lacking KIF4 Are Resistant to Apoptosis

Next, to analyze the role of KIF4 in postmitotic neurons, we generated *kif4*$^{+/Y}$ and *kif4*$^{-/Y}$ neurons by in vitro differentiation of ES cells. After an induction of neuronal differentiation, 90 percent of the cells turned into MAP2-positive neurons in both genotypes (Figure S3A). Further immunocytochemistry showed that these neurons were mainly glutamate positive, that some were GABA positive (Figures S4Aa and S4Ab), and that they expressed NMDA-receptor (subunit 2B; Figure S4Ba and S4Bb). Importantly, they did not express choline acetyltransferase (ChAT; Figure S4C). These results indicate that they have a property typical of neurons in the central nervous system, not of ones in peripheral nervous system. Between genotypes, there was no difference in cell morphology, expression of various neuronal markers, and in axon-dendrite polarity, suggesting that KIF4 is not essential for neuronal differentiation (Figures S3B and S4).

PARP-1 has been implicated in the mechanism of neuronal cell death (Nicoletti and Stella, 2003). Although a pathological overactivation of PARP-1 leads to cell death due to an energy deficit (Ha and Snyder, 2000), it has been suggested that a physiological activation of PARP-1 could protect neurons from apoptosis (Nicoletti and Stella, 2003). In this context, we compared survival between the genotypes of MAP2-positive cells kept in culture medium deprived of trophic factors (Weller et al., 1997; Ikeuchi et al., 1998; Putcha et al., 2002). The survival rate of MAP2-positive neurons was much higher in *kif4*$^{-/Y}$ cell cultures than in *kif4*$^{+/Y}$ cell cultures after 6 days deprivation of trophic factors (Figures 3A and S5). Nuclear staining using 4′,6-diamidino-2-phenylindole, dihydrochloride (DAPI) revealed a lower rate of apoptosis in *kif4*$^{-/Y}$ neurons to be responsible for the difference (Figure 3B). In the presence of a PARP-1 inhibitor (3-AB or 1,5-isoquinolinediol [DHIQ]), the percentage of apoptotic cell death of *kif4*$^{-/Y}$ neurons was increased to reach the level of *kif4*$^{+/Y}$ neurons (Figures 3A and 3B), indicating that the antiapoptotic resistance of *kif4*$^{-/Y}$ neurons depends on PARP-1 activity.

Next, we examined whether two well-known antiapoptotic pathways are related to PARP-1 activity. One is mediated by neuronal activity (Gallo et al., 1992; Franklin and Johnson, 1992) and the other by neurotrophic factors (Ferrari et al., 1989; Yuan and Yankner, 2000). The survival of *kif4*$^{+/Y}$ neurons increased to the level of *kif4*$^{-/Y}$ neurons, both by membrane depolarization induced by high potassium stimulation and by the addition of trophic factors (NGF + bFGF) into the medium (Figures 3A and 3B). The antiapoptotic effect of the membrane depolarization was blocked by PARP-1 inhibitors, but that of the trophic factors was not, in both *kif4*$^{+/Y}$ and *kif4*$^{-/Y}$ neurons (Figures 3A and 3B, respectively). These results suggest that PARP-1 activation is specifically related to the antiapoptotic pathway mediated by the depolarization of the membrane potentials of young neurons. In parallel with these experiments, we measured PARP-1 activity in *kif4*$^{+/Y}$ and in *kif4*$^{-Y}$ neurons before and after high potassium stimulation. In the *kif4*$^{-/Y}$ neurons, the high potassium treatment increased PARP-1 activity (Figures 3C and 3D). In contrast, PARP-1 activity in the *kif4*$^{-/Y}$ neurons was about 2-fold of that in *kif4*$^{+/Y}$ neurons before stimulation and was relatively unchanged after high potassium stimulation (Figures 3C and 3D). Taken together, we conclude that a lack of KIF4 results in the upregulation of PARP-1 activity and suggest that KIF4 controls neuronal cell survival by regulating PARP-1 activity.

KIF4/PARP-1 Complex Regulates Neuronal Cell Survival

To confirm the possible role of the KIF4/PARP-1 complex in support of neuronal survival, as suggested by experiments using ES cell-derived neurons, we applied an RNA interference (RNAi) knockdown approach to a primary culture of cerebellar granule cells (CGCs), a standardized model to study mechanisms of neuronal survival in vitro (Franklin and Johnson, 1992). High potassium treatment on these neurons activated PARP-1 (Figure S6Da) in a time-dependent manner (Figure S6Db) and supported cell survival by preventing apoptosis as described previously (Lin et al., 1997; Weller et al., 1997). This neuroprotective effect was blocked by a PARP inhibitor DHIQ (Figures S6A, S6B, and S6C), and prevention of cell death by trophic factors was not affected by the PARP inhibitor (Figures S6A, S6B, and S6C), as observed in neurons differentiated from ES cells.

A short interfering RNA (siRNA; 2388–2412) silenced PARP-1 in CGCs at 2.5 days after transfection (Figures 4A and 4B), whereas scrambled siRNA or noneffective siRNA (762–786) did not (Figure 4B). Specifically, in cells treated with siRNA (2388–2412), high potassium treatment failed to protect them from apoptotic cell death after removal of trophic factors (Figures 4C and 4D), resulting in a decreased number of live cells (Figures S7A and S7B). The effect of neurotrophic factors in support of cell survival was unaffected by knockdown of PARP-1 (Figures 4C, 4D, and S7).

Next, we knocked down KIF4 in CGCs by siRNA (2509–2533; Figure 4E). Treatment with siRNA (2509–2533), as well with KCl, increased nuclear labeling with anti-PAR antibody, demonstrating that PARP-1 was activated in CGCs (Figures 4F and 4H). Scrambled siRNA did not activate PARP-1 (Figures 4F and 4H). We monitored cell survival under the siRNA treatment. SiRNA (2509–2533) increased the number of live cells as well as did KCl stimulation (Figures 4G and 4I). This effect was sensitive to DHIQ (Figure 4J). In contrast, cell survival supported by trophic factors was not sensitive to DHIQ (Figure 4J).

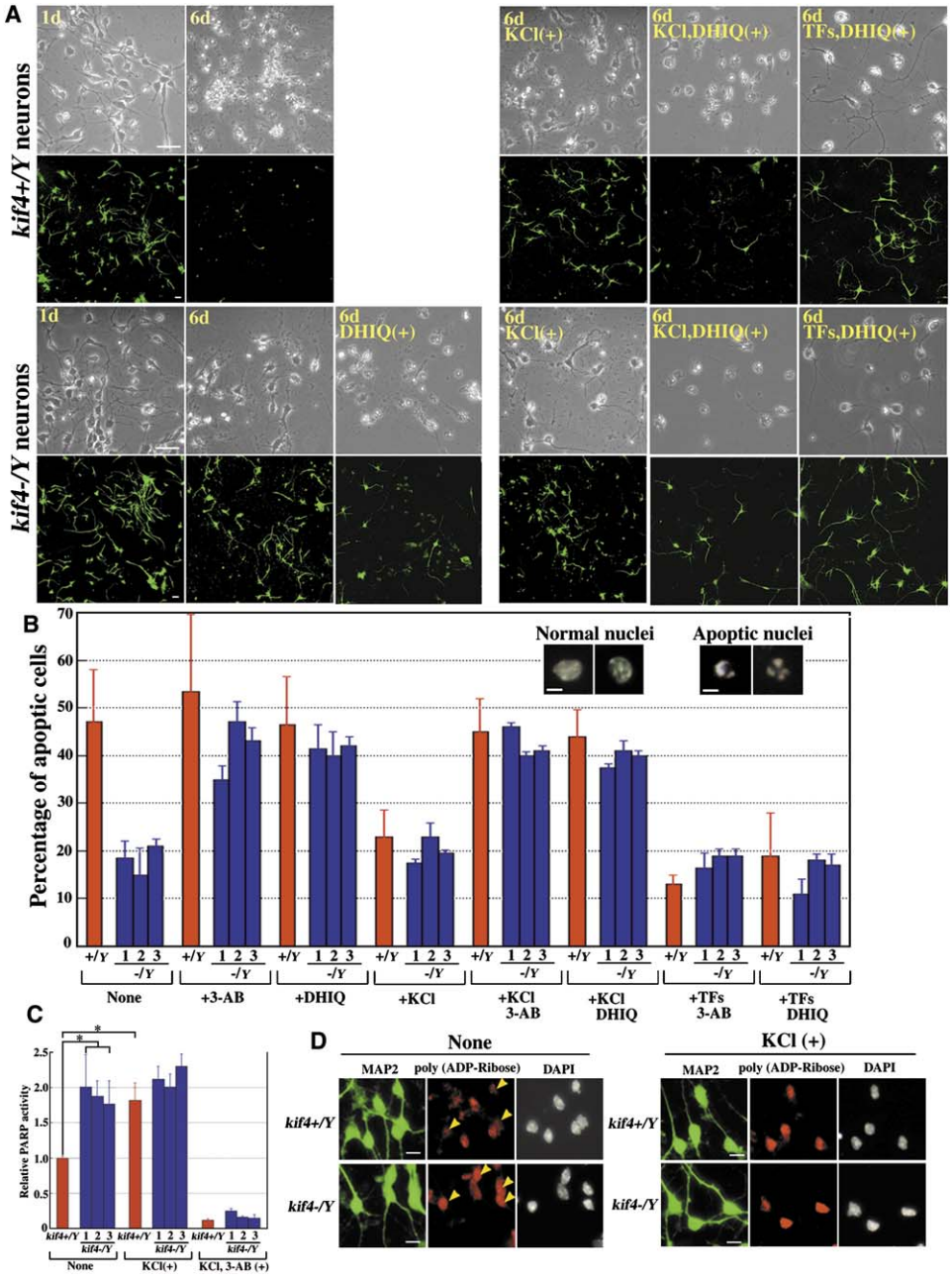

Figure 3. Neuronal Cell Death after Removal of Trophic Factors

(A) Phase contrast images and MAP2 immunolabeling of neurons at 1 and 6 days after removal of trophic factors. Bars = 20 μm.

(B) Percentage of apoptotic cells. Two days after deprivation of trophic factors with various stimuli as denoted at the bottom of the graph, the numbers of cells with condensed chromatin (shown in the upper panels; bars = 5 μm) per 1000 cells were counted. Three independent *kif4*$^{-/Y}$ clones were analyzed. Values (mean ± SD) were calculated from three experiments.

(C and D) PARP-1 activity of *kif4*$^{+/Y}$ and *kif4*$^{-/Y}$ neurons.

(C) PARP-1 activity of cell lysates collected 1 day after deprivation of trophic factors. After treatment with 50 mM KCl for 5min, the PARP-1 activity of *kif4*$^{+/Y}$ cell lysates significantly increases (*$p < 0.05$; t test). In contrast, the PARP-1 activity of *kif4*$^{-/Y}$ neurons was significantly higher than that of *kif4*$^{+/Y}$ before stimulation (*$p < 0.05$; t test), and is unchanged by KCl treatment. Addition of 3-AB suppresses PARP-1 activity. Mean ± SD is presented. Data were accumulated from five independent experiments.

(D) Immunolabeling of MAP2-positive cells with anti-PAR antibody before and after treatment with 50 mM KCl for 5 min. Fluorescence intensities of poly (ADP-ribose) labeling are higher in *kif4*$^{-/Y}$ cells than in *kif4*$^{+/Y}$ cells before treatment with KCl (arrowheads). Bars = 10 μm.

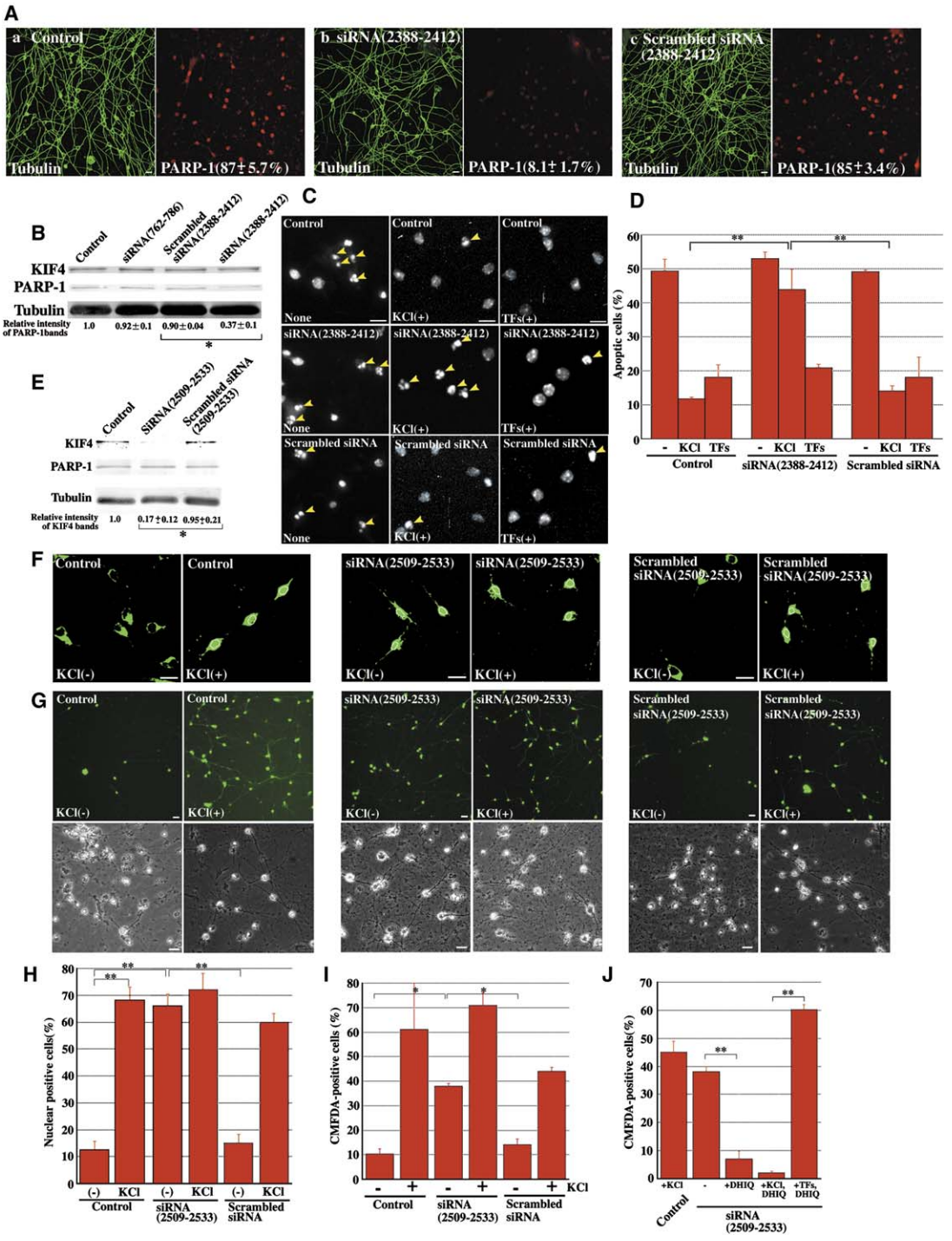

Figure 4. Knockdown by RNAi

(A–D) Knockdown of PARP-1.

(A) Immunostaining of CGCs at 2.5 days after the transfection of siRNAs is denoted in the panels. Control in (a) means a condition without siRNA. The percentages of PARP-1-positive cells are denoted at the bottom of the panels. Values (mean ± SD) were calculated from three experiments. The differences between (a) and (b) and between (b) and (c) are statistically significant ($p < 0.001$; t test). Bars = 20 μm.

(B) Immunoblotting of lysates. Values denoted at the bottom are the relative intensity of PARP-1 immunoreactivity calculated from three independent experiments. (*$p < 0.05$; t test).

(C) DAPI-staining of CGCs transfected with siRNAs. At day 2 after transfection, trophic factors were removed and cells kept in the conditions denoted at the bottom of panels for 4 days. Apoptotic cells are indicated by arrowheads. Bars = 20 μm.

Taken together, PARP-1 activation is an essential step in the pathway for neuronal survival induced by membrane depolarization, and this activation is negatively regulated by KIF4.

Support for Cell Survival Mediated by the KIF4/PARP-1 Complex Depends on Ca^{2+} Influx through the Voltage-Sensitive Ca^{2+} Channel

Next, we investigated calcium signaling in *kif4*$^{+/Y}$ and in *kif4*$^{-/Y}$ cells. KCl-induced membrane depolarization triggers an influx of Ca^{2+} into cytoplasm and nuclei through the L-type voltage-sensitive calcium channel (VSCC; Hardingham et al., 1998), and the nuclear calcium signal activates PARP-1 (Homburg et al., 2000). In both *kif4*$^{+/Y}$ and in *kif4*$^{-/Y}$ neurons, high potassium stimulation induces cytoplasmic and nuclear Ca^{2+} elevation (Figure 5A). When Ca^{2+} influx was blocked by nicardipine, a selective blocker for VSCC, high potassium treatment failed to support *kif4*$^{+/Y}$ cell survival (Figures 5Ba and 5Bb). On the other hand, survival of *kif4*$^{-/Y}$ cells stimulated by KCl was not affected by nicardipine treatment (Figures 5Ba and 5Bb). These observations indicated that Ca^{2+} influx is required for activity-dependent cell survival in *kif4*$^{+/Y}$ neurons and that *kif4*$^{-/Y}$ neurons are resistant to apoptosis even in the absence of an elevated Ca^{2+} level, possibly because of the persistent elevation of PARP-1 activity. In other words, regulation of PARP-1 activity by KIF4 is situated in the downstream of neuronal nuclear calcium influx.

KIF4 Is Dissociated from PARP-1 after Membrane Depolarization

Next, we focused on a possible change in the KIF4-PARP-1 interaction after membrane depolarization. Since a recent report has shown that membrane depolarization induces the automodification of PARP-1 by poly ADP-ribosylation through the influx of Ca^{2+} into nucleoplasm (Homburg et al., 2000), we first examined the effect of PARP-1 automodification on the binding of PARP-1 to KIF4 in vitro. Automodified PARP-1 did not bind to the KIF4-tail (Figure 5C). Next, we compared the binding of KIF4 to PARP-1 before and after KCl stimulation in vivo. High potassium stimulation decreased the amount of KIF4 immunoprecipitated by the PARP-1 antibody (Figure 5D). Addition of a calcium chelator *O,O′*-Bis(2-aminophenyl) ethyleneglycol-*N,N,N′,N′*-tetraacetic acid, tetraacetoxymethyl ester (BAPTA-AM) into the culture medium blocked the decrease (Figure 5D), indicating Ca^{2+} elevation is necessary for KIF4-PARP-1 dissociation. Along with this, automodified PARP-1 increased after KCl stimulation, which was inhibited by the PARP-1 inhibitor DHIQ (Figure 5E). These biochemical data demonstrate that KIF4 is dissociated from automodified PARP-1 after membrane depolarization.

We next monitored for possible changes in the cellular localization of KIF4 after KCl stimulation. Before stimulation, KIF4 is dominantly localized in the nucleus (Figure 5Fa). In contrast, after cells were treated with high potassium for 30 min, a considerable immunoreactivity of KIF4 was observed in neurites (Figures 5Fb and S8). This altered localization of KIF4 was blocked by the addition of BAPTA-AM (Figure 5Fc and S8) or the PARP-1 inhibitor DHIQ (Figures 5Fd and S8), indicating that the localization depends on Ca^{2+} and PARP-1 activity. The localization of PARP-1 did not change after depolarization (Figures 5Fe and 5Ff). The redistribution of KIF4 was also blocked by nocodazol, a microtubule-depolymerizing agent (Figures 5Ga, 5Gb, and S8), accompanied by an intermittent disruption of microtubules in neurites (Figures 5Gc and 5Gd) without affecting cell viability revealed by 5-chloromethylfluorescein diacetate (CMFDA), a fluorescent tracer that diffuse through the membranes of live cells (Figures 5Ga and 5Gb). Together, these data suggest that a microtubule-dependent motility of KIF4 underlies its translocation after depolarization. This activity-dependent translocation of KIF4 into cytoplasm and its inhibition by DHIQ and BAPTA-AM was also clearly observed in CGCs (Figure S9).

CaMKII Plays Pivotal Roles in the KIF4/PARP-1 Pathway

These events, nuclear Ca^{2+} elevation, activation of PARP-1, and translocation of KIF4 to cytoplasm, were reproduced by an alternative method of neuronal activation, electrical field stimulation to CGCs. With 50 Hz pulse stimuli, nuclear poly ADP-ribosylation accompanied with calcium elevation was induced (Figures 6A, 6Ba, and 6Bb) and translocation of KIF4 into cytoplasm was increased (Figures 6Ca and 6Cb). Using this system, we addressed the possible involvement of calcium-calmodulin kinase II (CaMKII) in the regulation of PARP-1 activity, inspired by a recent report showing that PARP-1 is activated by CaMKII phosphorylation (Ju et al., 2004). Both processes,

(D) Percentage of apoptotic cells. Values (mean ± SD) were calculated from three independent experiments. (**$p < 0.01$; t test).

(E–J) Knockdown of KIF4.

(E) Immunoblotting of lysates. Values denoted at the bottom are the relative intensity of KIF4 immunoreactivity calculated from three independent experiments. (*$p < 0.05$; t test).

(F) Immunolabeling by anti-PAR antibody for CGCs transfected with siRNA denoted at the top of each panel and subjected to various stimuli for 10 min denoted at the bottom. Control means without siRNA. White line circles indicate nuclei. Bars = 20 μm.

(G) CMFDA labeling and phase-contrast images of CGCs transfected with siRNAs targeted for KIF4. At 1 day after transfection, survival assay was started and cells were kept under the various conditions denoted at the bottom of the panels for 7 days. Bars = 20 μm.

(H) Statistical analysis of PAR-positive cells in nuclei after various stimuli denoted at the bottom of panel. Nuclear positive cells per 200 cells were counted for each experiment. Mean ± SD calculated from three experiments is presented. (**$p < 0.01$; t test).

(I and J) Percentages of living cells cultured under the various conditions for 7 days are denoted at the bottom of the panels. Values (mean ± SD) were calculated from three independent experiments. (*$p < 0.05$ and **$p < 0.01$; t test).

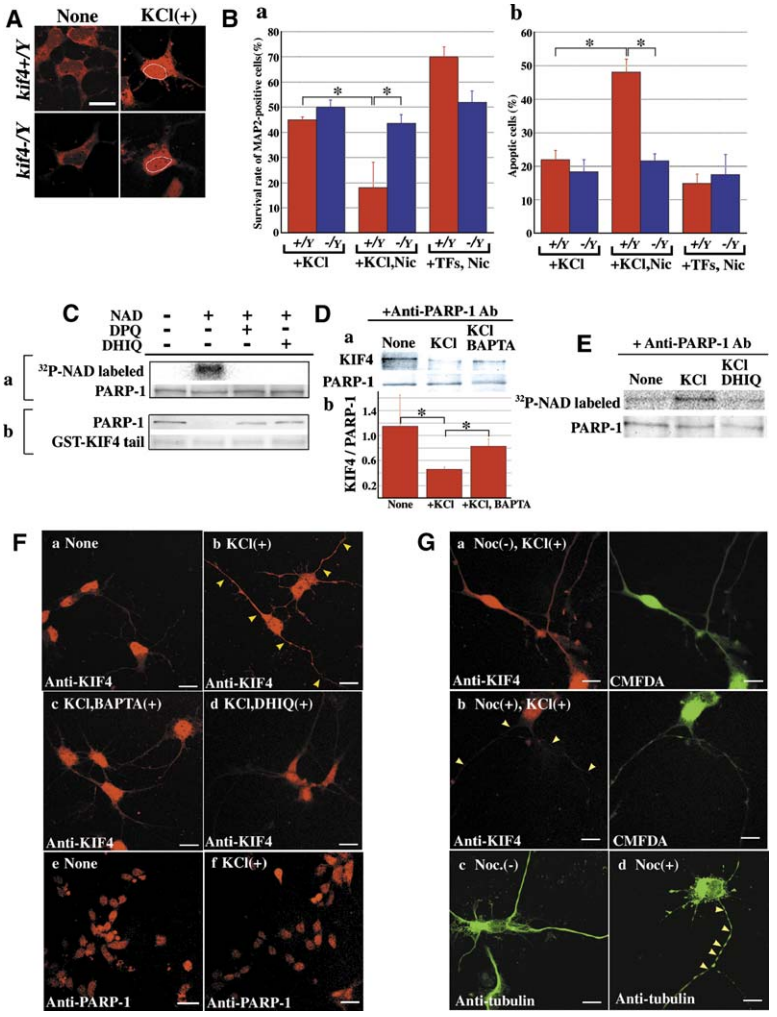

Figure 5. KIF4 Is Dissociated from PARP-1 and Moves to Neurites after Membrane Depolarization

(A) Before and after incubation with 25 mM KCl for 15 min, both *kif4*$^{+/Y}$ and *kif4*$^{-/Y}$ neurons were labeled with 5 μM Rhod2-AM, a calcium-sensitive fluorescent dye. White line circles show the area of nuclei. Bars = 10 μm.

(B) Effect of VSCC blocker nicardipine (Nic) on KCl-dependent survival of MAP2-positive cells. (a) Survival of MAP2-positive cells. (b) Percentages of apoptotic cells (mean ± SD) were calculated from three experiments using DAPI staining (*$p < 0.05$; t test).

(C–E) Activity-dependent dissociation of KIF4 from PARP-1.

(C) Effect of the automodification of PARP-1 on its binding to KIF4. Activated calf-thymus DNA (Scovassi et al., 1984) was added to each sample. (a) PARP inhibitors (DPQ and DHIQ) inhibit the ^{32}P-NAD-labeling of PARP-1 (upper panel). Immunoblotting using anti-PARP-1 antibody (lower panel). (b) Binding of PARP-1 with GST-KIF4 tail. Automodified PARP-1 does not bind to KIF4 tail.

(D) (a) Interaction between KIF4 and PARP-1 in depolarized neurons. After depolarization in the presence or absence of BAPTA-AM, lysates were collected and immunoprecipitation performed using anti-PARP-1 antibody. (b) The KIF4/PARP-1 ratio of the intensity of the immunoblots (mean ± SD; *$p < 0.05$; t test).

(E) Increased automodification of PARP-1 in depolarized neurons. ^{32}P-NAD-labeled PARP-1 is immunoprecipitated.

(F) Immunolabeling of neurons with KIF4 (a–d) and PARP-1 (e and f) antibodies before and after depolarization. (a) Cells before depolarization. (b) Cells treated with 50 mM KCl. Immunoreactivity of KIF4 in neurites is indicated by arrowheads. (c) Cells treated with 50 mM KCl + 6 μM BAPTA-AM (a calcium chelator). (d) Cells treated with 50 mM KCl + 50 μM DHIQ. In (c) and (d), redistribution of KIF4 was inhibited. (e and f) Immunolabeling of neurons before (e) and after (f) depolarization using anti-PARP-1 antibody.

(G) (a and b) Nocodazol (Noc)-treated cells were incubated with 50 mM KCl for 25 min and immunolabeled by anti-KIF4 antibody. Nocodazol treatment decreases KIF4 immunoreactivity in neurites (arrowheads in [b]). CMFDA labeling in (a) and (b) demonstrates that nocodazol treatment did not affect cell viabilities. (c and d) Effect of nocodazol. Neurons treated with 2.5 μM nocodazol for 1 hr show an intermittent disruption of microtubules in neurites (d, arrowheads).

PARP-1 activation and KIF4 translocation in CGCs after field stimulation (Figures 6Bb, 6Bc, 6Cb, and 6Cc) or high potassium stimulation (data not shown), were blocked by CaMKII inhibitor KN-62. When activated by membrane depolarization, PARP-1 was phosphorylated (Figure 6Da). This phosphorylation, PARP-1 automodification, and PARP-1/KIF4 dissociation are sensitive to KN-62 (Figures 6Da, 6Db, and 6Dc), suggesting that these events are under the control of CaMKII.

Overexpression of Headless KIF4 Promotes Neuronal Cell Death in Developing Brain

Finally, to confirm the role of KIF4 in the developing mouse brain, we overexpressed *kif4* vectors by in utero electroporation. For an assessment of the function of PARP-1 binding (tail) domain in controlling neuronal cell death, we prepared two types of vectors: headless and tailless *kif4* (Figure 7A). Each vector was designed to express truncated KIF4 and GFP in a bicistronic fashion mediated by internal ribosome entry site (IRES; Figure 7A). When transfected into cultured cells, headless *kif4* blocked PARP-1 activation induced by H_2O_2, but tailless *kif4* did not, as described above (Figure 2Bc). At 3 days after in utero electroporation, the GFP signal was detected in neurons situated in the hippocampal CA1 field (Figure 7B). Enhancement in immunoreactivity against KIF4 was confirmed in GFP-positive neurons (Figure 7C). We compared numbers of GFP-positive neurons per area between headless- and tailless- transfected brain sections. At 3 days after electroporation, there was no difference (Figures 7D and 7E),

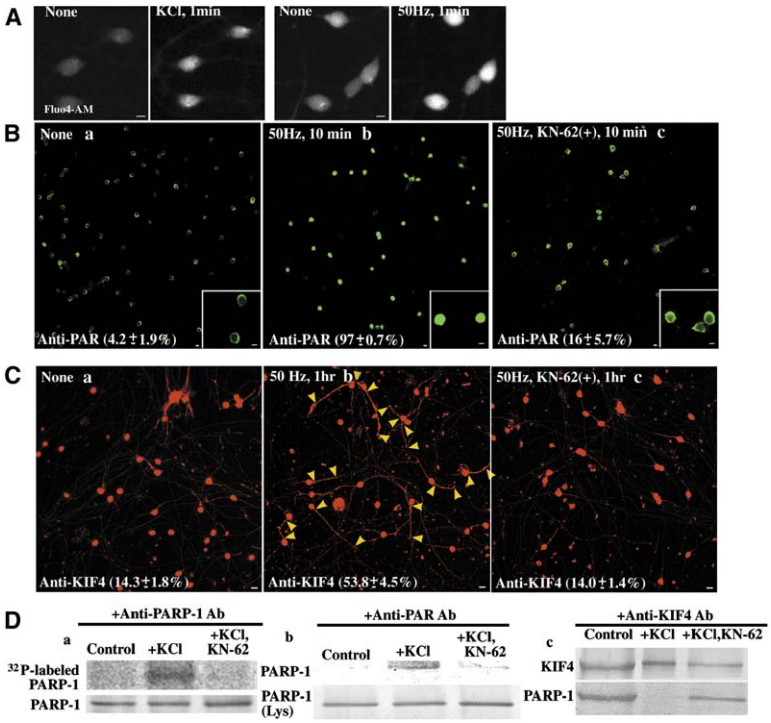

Figure 6. CaMKII Mediates Depolarization-Dependent PARP-1 Activation and Dissociation of the KIF4/PARP-1 Complex

(A–C) Electrical stimulation applied to CGCs.

(A) Calcium imaging using fluo-4 AM for CGCs before and after stimulation is denoted at the top of each panel. Bars = 10 μm.

(B) Immunolabeling by anti-PAR antibody after subjecting to the stimuli denoted at the top of each panel. Bars = 10 μm. Values mean percentages of nuclear positive cells per 200 cells. Mean ± SD calculated from three experiments is presented. (a and b: **p < 0.01; b and c: **p < 0.01; t test).

(C) Cellular localization of KIF4 after field stimulation. KIF4 was immunolabeled after subjecting to the various stimuli denoted at the top of each panel. The elevated immunoreactivity of KIF4 in neurites is indicated by arrowheads. Values mean percentages (mean ± SD) of cells with illuminated neurites per 200 cells calculated from three experiments. (a and b: **p < 0.01; b and c: **p < 0.01; t test). Bars = 10 μm.

(D) CaMKII-dependent phosphorylation of PARP-1 in CGCs. (a) Labeling of PARP-1 with [^{32}P]-orthophosphate before and after depolarization (upper panel). The phosphorylation of PARP-1 was blocked by KN-62. Bottom panel shows immunoblotting of immunoprecipitates using anti-PARP-1 antibody. (b) Automodification of PARP-1. Cells were subjected to the various stimuli denoted at the top of the panel, and lysates were immunoprecipitated using anti-PAR antibody and immunoblotted with anti-PARP-1 antibody. (c) KIF4 is dissociated from PARP-1 after KCl treatment. KN-62 blocks this dissociation.

whereas at 6–8 days after, the numbers of GFP-positive neurons in sections transfected with the headless *kif4* gene were lower than in ones with the tailless *kif4* gene (Figures 7D and 7E), suggesting the effect of the KIF4 tail domain to enhance cell death. We examined the morphology of GFP-positive neurons in detail at 8 days after electroporation and found that the neurons transfected with headless *kif4* gene lacked neurites and showed condensed nuclear chromatin (Figure 7Fa), whereas the morphology of neurons transfected with tailless *kif4* gene was intact (Figure 7Fb). These results indicate that overexpression of the KIF4 tail domain enhanced cell death in the developing brain possibly by the inhibition of PARP-1 activity.

DISCUSSION

The Role of KIF4 in Brain Development

Juvenile neurons die in a physiological process during development that, in cooperation with the regulation of cell proliferation, contributes to the control of cell numbers. Programmed cell death plays a major part in this process (Yuan and Yankner, 2000) and is regulated by neuronal activity and successive Ca^{2+} signaling. We found that the regulating mechanism for this activity-dependent programmed cell death is mediated by the KIF4/PARP-1 complex, a combination of a kinesin superfamily protein and a nuclear enzyme.

In spite of its abundant expression, little is known as regards KIF4 and its role in postmitotic neurons (Sekine et al., 1994). Through biochemical, cell-biological, and molecular-genetic approaches, we demonstrated an unexpected role for KIF4 in the control of activity-dependent cell survival of juvenile neurons. Our data suggest the concept wherein the C terminus of the kinesin superfamily protein, which is regarded as a cargo binding domain in other KIFs (Hirokawa and Takemura, 2005), serves as a controlling module for the enzymatic activity of its binding protein. This might be an example of "domain shuffling" during protein evolution, where domains with different functions are accidentally combined together to generate a variety of new molecules.

The results suggest a model of the sequential events in the control of activity-dependent cell survival that are presented schematically in Figure 7G. (1) In a steady state, KIF4 binds to PARP-1 and suppresses PARP-1 activity. Cells are then prone to apoptotic death. (2) Membrane depolarization triggers Ca^{2+} influx into nucleoplasm via the

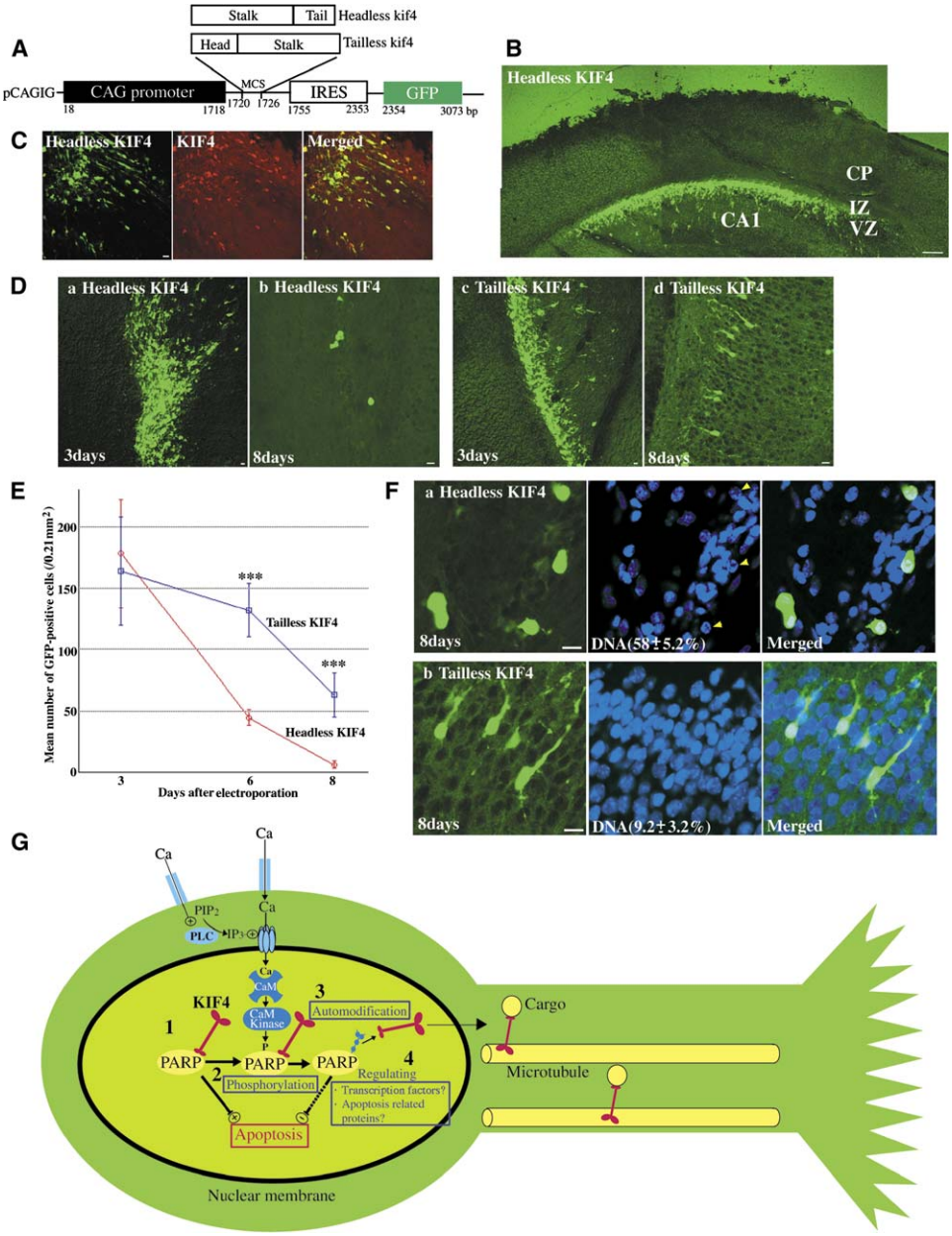

Figure 7. Overexpression of Headless KIF4 Promotes Neuronal Cell Death in Developing Brain

(A–F) In utero electroporation of KIF4 expression vectors.

(A) Construction of the expression vectors. Headless or tailless *kif4* genes were inserted in the downstream of the CAG promoter for bicistronic coexpression with GFP. MCS: multicloning sites.

(B) A typical view of GFP expression in cerebrum transfected with the headless *kif4* construct. Coronal section of whole brain at 3 days after electroporation (postnatal day 1) is shown. Bars = 100 μm.

(C) Coexpression of GFP with KIF4. KIF4 is illuminated by immunolabeling with anti-KIF4 polyclonal antibody. Bars = 10 μm.

(D) GFP-positive cells in brain sections transfected with headless *kif4* (a and b) or tailless *kif4* (c and d). Sections photographed at 3 (a and c) and 8 (b and d) days after electroporation are shown. Bars = 10 μm.

(E) Statistical analysis. An area of about 3.8 mm^2 of each section was examined and the mean number (mean ± SD) of GFP-positive cells per 0.21 mm^2 (corresponding to a visual field of 20× objective) are shown. To calculate each point on the graph, 18 sections obtained from two independent electroporation were examined. ***$p < 0.001$; t test.

(F) Cellular morphology of GFP-positive neurons. GFP signal (left panels), DNA labeling (middle panel), and merged (right panel) of sections transfected with headless (a) and tailless (b) *kif4* genes. Arrowheads show nucleus with condensed chromatin. Values at the bottom of the middle panels mean percentages (mean ± SD) of GFP-positive cells with condensed chromatin. Forty cells observed in 18 sections (obtained from two electroporations) were used to calculate each value. The difference between the values was statistically significant, **$p < 0.01$; t test). Bars = 10 μm.

IP_3 receptor localized on nuclear membrane. Elevated Ca^{2+} makes a complex with calmodulin (CaM) and activates CaMKII, which phosphorylates PARP-1. (3) These events trigger automodification of PARP-1 (Homburg et al., 2000) . (4) KIF4 is dissociated from poly ADP-ribosylated PARP-1 and moves into neurites, where it can transport some cargoes to the distal part of neurites in a microtubule-dependent manner. These observations clearly show a role for KIF4 as a molecular motor in cytoplasm; indeed, a previous study reported that KIF4 is involved in the transport of L1, an adhesion molecule required for axon formation (Peretti et al., 2000). Possibly, KIF4 may transport cargoes required for neuronal development, such as L1, after dissociation from PARP-1 in an activity-dependent manner (Figure 7G). Considering the accumulated evidence, an intriguing possibility arises that KIF4 has a dual role in the nucleus and cytoplasm of neurons and contributes to brain development, although further characterization of the cargo of KIF4 is still necessary.

As for the function of KIF4 in proliferating cells, several candidates for a KIF4 homolog have been identified and implicated in mitosis (Wang and Adler, 1995; Vernos et al., 1995; Oh et al., 2000; Lee et al., 2001). Contrary to expectations, ES cells lacking KIF4 divided normally, showing that at least in murine ES cells KIF4 was not essential for mitotic cell division (Figure S2). This could be because there is a redundancy among KIF4 and some other murine KIFs in mitosis or because the candidates are not true homologs of murine KIF4 but rather variants with different functions from that of murine KIF4. Supporting this view, the homology of the tail domain is significantly low among murine KIF4, chromokinesin, XKLP1, and hKIF4A.

PARP-1 Prevents Apoptosis

PARP-1 is a multifunctional protein that has been implicated in the control of cell death (D'Amours et al., 1999). In pathological conditions such as brain ischemia or NMDA receptor-mediated neurotoxicity, an overactivation of PARP-1 induces cell death through the acute consumption of intracellular energy sources such as ATP and NAD (Didier et al., 1994; Mandir et al., 2000; Garnier et al., 2003). It is also well known that PARP-1 is cleaved by caspase-3 in the late stage of apoptosis (Kawahara, et al., 1998; Gilliams-Francis et al., 2003).

Aside from these findings, recent studies have focused on PARP-1 activation in physiological condition. In neurons, PARP-1 is activated by a Ca^{2+}-mediated signal induced by membrane depolarization (Figure 7G; Homburg et al., 2000) and poly ADP-ribosylation mediates long-term memory in *Aplysia* sensitized by repetitive stimuli (Cohen-Armon et al., 2004). In our study, knock-down experiments using RNAi (Figure 4) and pharmacological blocking (Figures 3 and S5) of PARP-1 activity directly revealed another important aspect of PARP-1's physiological roles: its activation protects juvenile neurons from apoptotic cell death. It is notable that both memory formation and neuroprotection require Ca^2 influx induced by membrane depolarization, raising the possibility that both processes share the same mechanism, although details of how membrane depolarization protects juvenile neurons from apoptosis is not fully understood (Franklin and Johnson, 1992; Kocsis et al., 1994; Weller et al., 1997; Lin et al., 1997; Hardingham et al., 1998; Malviya and Rogue, 1998).

So, how does PARP-1 participate in this neuroprotective pathway? One possibility is that it induces the expression of antiapoptotic genes, acting as a coactivator of various transcription factors (Kraus and Lis, 2003), such as nuclear factor κB (NF-κB). In support of this view, previous studies have reported that NF-κB is activated by membrane depolarization (Kaltschmidt et al., 1995) and also by PARP-1 (Chang and Alvarez-Gonzalez, 2001; Chiarugi and Moskowitz, 2003) and that it supports the survival of neurons by inducing expressions of several antiapoptotic genes such as *inhibitors of apoptosis protein 1* (*c-IAP-1*), *c-IAP-2*, and *Bcl-XL* (Bhakar et al., 2002).

In the context of transcriptional regulation, activated PARP-1 is reported to regulate neurogenic gene expression under the control of calcium signaling (Ju et al., 2004). It is noteworthy that CaMKII plays a critical part in this process, as it does in the neuroprotective pathway mediated by the KIF4/PARP-1 complex. On the other hand, KIF17b, another kinesin-related protein, is reported to participate in transcriptional regulation through interacting with a transcriptional coactivator in male germ cells (Macho et al., 2002). Considering the possibility that KIF4 also regulates gene expression related to apoptosis via its binding with PARP-1 (Figure 7G), detection of genes with their expression under the control of the KIF4-PARP-1 interaction is an important subject for future research.

EXPERIMENTAL PROCEDURES

Production of Recombinant Protein and GST Pull-Down

GST-KIF4 tail (amino acid no. 1005–1231) was produced by an *E. coli* BL21 RIL expression system (Novagen) using standard techniques (Kaelin et al., 1992). For GST pull-down, brain high-speed supernatant from 5-day-old mice was applied to KIF4 tail conjugated glutathione beads (Pharmacia). After an overnight incubation at 4°C, eluents were collected sequentially by adding NaCl (1.0, 2.0 M) buffer. P110 was excised from the gel and subjected to peptide sequencing (Aproscience Corp.) and mass spectrometry (Genomic Solutions, Inc.).

In Vitro Protein Binding Assay

Six micrograms of GST-KIF4 tail conjugated with Sepharose beads was incubated with 2 μg of partially purified PARP (Biomol. Inc) in a reaction buffer (20 mM Tris-HCl [pH 7.4], 0.15 M NaCl, 100 μg/ml BSA, protease inhibitors [Roche]) at 4°C for 6 hr in the presence or absence

(G) Schematic model of the involvement of KIF4 in the regulation of the survival of developing neurons. (1) KIF4 binds to PARP-1 and inhibits PARP-1 activity. (2) After membrane depolarization, elevated Ca^{2+} activates CaMKII, which phosphorylates PARP-1. (3) PARP-1 is automodificated (Homburg et al., 2000). (4) KIF4 is dissociated from poly ADP-ribosylated PARP-1 and moves into neurites. Upregulated PARP-1 activity promotes expression of genes and modifies nuclear proteins to support cell survival.

of a final 50 μg/ml calf thymus DNA (Sigma) and analyzed by immunoblotting. To examine DNA-protein binding, 7 μg of purified GST-KIF4 or 1 μg of purified PARP was incubated in the reaction buffer described above with 25 μl of 2 mg/ml DNA-cellulose (Pharmacia) at 4°C for 6 hr and analyzed by immunoblotting.

Measurement of PARP-1 Activity

Biochemical measurement of PARP-1 activity was performed according to a reported method (Schraufstätter et al., 1988) as follows: 2 μl of 2 μM nicotinamide-adenine dinucleotide, [adnine-2,8-^{3}H] (NEN) was added to the cell suspension and incubated at 25°C for 20 min. The radioactivity of the acid-insoluble material collected as precipitates was counted using a liquid scintillation counter.

Poly ADP-Ribosylation of PARP-1

Four microliters of 10 μM ^{32}P-NAD was added to the neuronal cell culture and incubated for 30 min. KCl (50 mM) was added and further incubated for 30 min. Lysate was then collected and applied for anti-PARP-1 immunoprecipitation. The radioactivity of ^{32}P-NAD-labeled PARP-1 was detected by autoradiography.

RNAi

siRNA (stealth RNA) directed against PARP-1 and KIF4 were purchased from Invitrogen. CGCs were transfected with siRNA using Lipofectamine 2000 (Invitrogen) according to the manufacturer's instructions. The nucleotide sequences of the siRNA were as follows: siRNA targeted for PARP-1—siRNA (762–786), 5′-AAGCUUACUAUACUUAUCUGUCUCC-3′; siRNA (2388–2412), 5′-AAGACUAUAGGCCACCUCGAUGUCC-3′; scrambled siRNA (2388–2412), 5′-AAGGUAUAUCCGGACCACAGCUUCC-3′; siRNA targeted for KIF4—siRNA (2509–2533), 5′-TTACGACGGCGCTCACTCAACTTGG-3′; scrambled siRNA (2509–2533), 5′-TTACTGCGCAGCGCTCTCAAACTGG-3′.

Survival Assay of CGCs

At day 1 after plating (8×10^4 cells/cm^2), the medium was changed to mN3 medium without NGF and bFGF. According to each of the experimental conditions, cells were maintained in the presence or absence of KCl (25 mM), DHIQ (50 μM), or trophic factors (NGF [100 ng/ml] + basic FGF [5 ng/ml]). After 6 days, cells were labeled with 2.5 μM CMFDA (Molecular Probes), and numbers and densities of CMFDA-positive cells were calculated. DAPI staining was performed at day 5 to calculate the number and density of apoptotic cells. For RNAi experiments, CGCs (8×10^4 cells/cm^2 for PARP-1 knockdown, 4×10^4 cells/cm^2 for KIF4 knockdown) transfected with the siRNAs were kept for two days in N3FL medium containing bFGF and NGF, and then survival assay was started by the removal of trophic factors.

Field Stimulation

The method for electrical stimulation of CGCs was essentially that described by Ozaki et al. (2004). In brief, CGCs were subjected to electrical stimulation using dish electrodes (custom designed by Unique Medical Co. Ltd). Pulses were generated by a stimulator (Master-8, A.M.P. Instruments Ltd or SEN-7203, Nihon Kohden Ltd). After rectangular pulses of alternating polarity (0.2 ms width and 0.5–5 V intensity) at 50 Hz were applied to CGCs in mN3 medium, CGCs were immunolabeled using anti-PAR or anti-KIF4 antibody.

Phosphorylation Assay

CGCs grown in mN_3 medium were supplemented with phosphate-free DMEM (Gibco) for 1.5 hr and labeled with ^{32}P-orthophosphate (Amersham Biosciences, 10 mCi/ml) for 1.5 hr. CGCs were then incubated with 50 mM KCl in the presence or absence of 5 μM KN-62 (Seikagaku Corporation). Lysate was collected using TritonX-100 and 50 nM okadaic acid (Sigma) containing buffer and subjected to immunoprecipitation using anti-PARP-1 antibody. Immunoprecipitates were electrophoresed and the gel exposed to an imaging plate.

In Utero Electroporation

The method for in utero electroporation was essentially that described by Tabata and Nakajima [2001]. Uterine horns of pregnant mice at E16 were exposed, and 1–2 μg of plasmid solution was injected into the lateral ventricle with a glass micropipette. The embryo in the uterus was placed between the tweezers-type electrode, which has 5 mm diameter disc electrodes at the tip (CUY650-5; Tokiwa Science). Electrical pulses (40 V and later; 50 ms) were charged five times at intervals of 950 ms with an electroporator (ECM830; BTX, a division of Genetronics, Inc.). Uterine horns were then placed back into the abdominal cavity to allow the embryos to continue normal development.

Supplemental Data

Supplemental Data include nine figures and Supplemental Experimental Procedures and can be found with this article online at http://www.cell.com/cgi/content/full/125/2/371/DC1/.

ACKNOWLEDGMENTS

We thank Dr. Miwa (University of Tsukuba) for the 10H antibody, Dr. Ozaki (University of Waseda) for kind technical advice for field stimulation, and Dr. Gotoh (University of Tokyo) for providing expression vectors and technical advice for in utero electroporation. We also thank Y. Okada for help and suggestions. This work was supported by a Center of Excellence grant from the Ministry of Education, Culture, Sports, Science and Technology of Japan to N.H. and a postdoctoral fellowship from Japanese Society for the Promotion of Science to R.M.

Received: March 1, 2004
Revised: December 1, 2005
Accepted: February 2, 2006
Published: April 20, 2006

REFERENCES

Aizawa, H., Sekine, Y., Takemura, R., Zhang, Z., Nangaku, M., and Hirokawa, N. (1992). Kinesin family in murine central nervous system. J. Cell Biol. *119*, 1287–1296.

Althaus, F.R., and Richter, C. (1987). ADP-ribosylation of proteins. Enzymology and biological significance. Mol. Biol. Biochem. Biophys. *37*, 1–237.

Bhakar, A.L., Tannis, L.L., Zeindler, C., Russo, M.P., Jobin, C., Park, D.S., MacPherson, S., and Barker, P.A. (2002). Constitutive nuclear factor-κB activity is required for central neuron survival. J. Neurosci. *22*, 8466–8475.

Chang, W.J., and Alvarez-Gonzalez, R. (2001). The sequence-specific DNA binding of NF-κB is reversibly regulated by the automodification reaction of poly (ADP-Ribose) polymerase-1. J. Biol. Chem. *276*, 47664–47670.

Chiarugi, A., and Moskowitz, M.A. (2003). Poly (ADP-ribose) polymerase-1 activity promotes NF-kappaB-driven transcription and microglial activation: implication for neurodegenerative disorders. J. Neurochem. *85*, 306–317.

Cohen-Armon, M., Visochek, L., Katzoff, A., Levitan, D., Susswein, A.J., Klein, R., Valbrun, M., and Schwartz, J.H. (2004). Long-term memory requires polyADP-ribosylation. Science *304*, 1820–1822.

D'Amours, D., Desnoyers, S., D'Silva, I., and Poirier, G.G. (1999). Poly(ADP-ribosyl)ation reactions in the regulation of nuclear functions. Biochem. J. *342*, 249–268.

Didier, M., Mienville, J.M., Soubrie, P., Bockaert, J., Berman, S., Bursztajn, S., and Pin, J.P. (1994). Plasticity of NMDA receptor expression during mouse cerebellar granule cell development. Eur. J. Neurosci. *6*, 1536–1543.

Ferrari, G., Minozzi, M.C., Toffano, G., Leon, A., and Skaper, D. (1989). Basic growth factor promotes the survival and development of mesencephalic neurons in culture. Dev. Biol. *133*, 140–147.

Franklin, J.L., and Johnson, E.M., Jr. (1992). Suppression of programmed neuronal death by sustained elevation of cytoplasmic calcium. Trends Neurosci. *15*, 501–508.

Gallo, V., Giovannini, C., and Levi, G. (1992). Depression by sodium ions of calcium uptake mediated by non-N-methyl-D-aspartate receptors in cultured cerebellar neurons and correlation with evoked D-[3H]aspartate release. J. Neurochem. *58*, 406–415.

Garnier, P., Ying, W., and Swanson, R.A. (2003). Ischemic preconditioning by caspase cleavage of poly(ADP-ribose) polymerase-1. J. Neurosci. *23*, 7967–7973.

Gilliams-Francis, K.L., Quaye, A.A., and Naegele, J.R. (2003). PARP cleavage, DNA fragmentation, and pyknosis during excitotoxin-induced neuronal death. Exp. Neurol. *184*, 359–372.

Griesenbeck, J., Ziegler, M., Tomilin, N., Schweiger, M., and Oei, S.L. (1999). Stimulation of the catalytic activity of poly(ADP-ribosyl) transferase by transcription factor Yin Yang 1. FEBS Lett. *433*, 20–24.

Ha, H.C., and Snyder, S.H. (2000). Poly(ADP-ribose) polymerase-1 in the nervous system. Neurobiol. Dis. *7*, 225–239.

Hardingham, G.E., Cruzalegui, F.H., Chawla, S., and Bading, H. (1998). Mechanisms controlling gene expression by nuclear calcium signals. Cell Calcium *23*, 131–134.

Hirokawa, N. (1998). Kinesin and dynein superfamily proteins and the mechanism of organelle transport. Science *279*, 519–526.

Hirokawa, N., and Takemura, R. (2005). Molecular motors and mechanisms of directional transport in neurons. Nat. Rev. Neurosci. *6*, 201–214.

Homburg, S., Visochek, L., Moran, N., Dantzer, F., Priel, E., Asculai, E., Schwartz, D., Rotter, V., Dekel, N., and Cohen-Armon, M. (2000). A fast signal-induced activation of poly (ADP-ribose) polymerase: a novel downstream target of phospholipase c. J. Cell Biol. *150*, 293–307.

Ikeuchi, T., Shimoke, K., Kubo, T., Yamada, M., and Hatanaka, H. (1998). Apoptosis-inducing and -preventing signal transduction pathways in cultured cerebellar granule neurons. Hum. Cell *11*, 125–140.

Ju, B.G., Solum, D., Song, E.J., Lee, K.J., Rose, D.W., Glass, C.K., and Rosenfeld, M.G. (2004). Activating the PARP-1 sensor component of the Groucho/TLE1 corepressor complex mediates a CaMKinaseII δ-dependent neurogenic gene activation pathway. Cell *119*, 815–829.

Kaelin, W.G., Jr., Krek, W., Sellers, W.R., Decaprio, J.A., Ajchenbaum, F., Fuchs, C.S., Chittenden, T., Li, Y., Farnham, P.J., Blanar, M.A., et al. (1992). Expression cloning of a cDNA encoding a retinoblastoma-binding protein with E2F-like properties. Cell *70*, 351–364.

Kaltschmidt, C., Kaltschmidt, B., and Baeuerle, P.A. (1995). Stimulation of ionotropic glutamate receptors activates transcription factor NF-κB in primary neurons. Proc. Natl. Acad. Sci. USA *92*, 9618–9622.

Kawahara, A., Enari, M., Talanian, R.V., Wong, W.W., and Nagata, S. (1998). Fas-induced DNA fragmentation and proteolysis of nuclear proteins. Genes Cells *3*, 297–306.

Kocsis, J.D., Rand, M.N., Lankford, K.L., and Waxman, S.G. (1994). Intracellular calcium mobilization and neurite outgrowth in mammalian neurons. J. Neurobiol. *25*, 252–264.

Kraus, W.L., and Lis, J.T. (2003). PARP goes transcription. Cell *113*, 677–683.

Lawrence, C.J., Dawe, R.K., Christie, K.R., Cleveland, D.W., Dawson, S.C., Endow, S.A., Goldstein, L.S., Goodson, H.V., Hirokawa, N., Howard, J., et al. (2004). A standardized kinesin nomenclature. J. Cell Biol. *167*, 19–22.

Lee, Y.M., Lee, S., Lee, E., Shin, H., Hahn, H., Choi, W., and Kim, W. (2001). Human kinesin superfamily member 4 is dominantly localized in the nuclear matrix and is associated with chromosomes during mitosis. Biochem. J. *360*, 549–556.

Lin, W.W., Wang, C.W., and Chuang, D.M. (1997). Effect of depolarization and NMDA antagonists on the role survival of cerebellar granule cells: a pivotal role for protein kinase C isoforms. J. Neurochem. *68*, 2577–2586.

Macho, B., Brancorsini, S., Fimia, G.M., Setou, M., Hirokawa, N., and Sassone-Corsi, P. (2002). CREM-dependent transcription in male germ cells controlled by a kinesin. Science *298*, 2388–2390.

Malviya, A.N., and Rogue, P.J. (1998). "Tell me where is calcium bred": Clarifying the roles of nuclear calcium. Cell *92*, 17–23.

Mandir, A.S., Poitras, M.F., Berliner, A.R., Herring, W.J., Guastella, D.B., Feldman, A., Poirier, G.G., Wang, Z.Q., Dawson, T.M., and Dawson, V.L. (2000). NMDA but not non-NMDA excitotoxicity is mediated by poly(ADP-ribose) polymerase. J. Neurosci. *20*, 8005–8011.

Nakagawa, T., Setou, M., Seog, D., Ogasawara, K., Dohmae, N., Takio, K., and Hirokawa, N. (2000). A novel motor, KIF13A, transports mannose-6-phosphate receptor to plasma membrane through direct interaction with AP-1 complex. Cell *103*, 569–581.

Nicoletti, V.G., and Stella, A.M. (2003). Role of PARP under stress conditions: cell death or protection? Neurochem. Res. *28*, 187–194.

Oh, S., Hahn, H., Torrey, T.A., Shin, H., Choi, W., Lee, Y.M., Morse, H.C., and Kim, W. (2000). Identification of the human homologue of mouse KIF4, a kinesin superfamily motor protein. Biochim. Biophys. Acta *1493*, 219–224.

Ozaki, M., Itoh, K., Miyakawa, Y., Kishida, H., and Hashikawa, T. (2004). Protein processing and releases of neuregulin-1 are regulated in an activity-dependent manner. J. Neurochem. *91*, 176–188.

Peretti, D., Peris, L., Rosso, S., Quiroga, S., and Caceres, A. (2000). Evidence for the involvement of KIF4 in the anterograde transport of L1-containing vesicles. J. Cell Biol. *149*, 141–152.

Putcha, G.V., Harris, C.A., Moulder, K.L., Easton, R.M., Thompson, C.B., and Johnson, E.M., Jr. (2002). Intrinsic and extrinsic pathway signaling during neuronal apoptosis: lessons from the analysis of mutant mice. J. Cell Biol. *157*, 441–453.

Schraufstätter, I.U., Halsey, W.A., Jr., Hyslop, P.A., and Cochrane, C.G. (1988). In vitro models for the study of oxidant-induced injury of cells in inflammation. Methods Enzymol. *163*, 328–339.

Scovassi, A.I., Stefanini, M., and Bertazzoni, U. (1984). Catalytic activities of human poly(ADP-ribose) polymerase from normal and mutagenized cells detected after sodium dodecyl sulfate-polyacrylamide gel electrophoresis. J. Biol. Chem. *259*, 10973–10977.

Sekine, Y., Okada, Y., Noda, Y., Kondo, S., Aizawa, H., Takemura, R., and Hirokawa, N. (1994). A novel microtubule-based motor protein (KIF4) for organelle transports, whose expression is regulated developmentally. J. Cell Biol. *127*, 187–201.

Tabata, H., and Nakajima, K. (2001). Efficient in utero gene transfer system to the developing mouse brain using electrporation: visualization of neuronal migration in the developing cortex. Neuroscience *103*, 865–872.

Tulin, A., and Spradling, A. (2003). Chromatin loosening by poly(ADP)-ribose polymerase (PARP) at Drosophila puff loci. Science *299*, 560–562.

Vernos, I., Raats, J., Hirano, T., Heasman, J., Karsenti, E., and Wylie, C. (1995). Xklp1, a chromosomal *Xenopus* kinesin-like protein essential for spindle organization and chromosome positioning. Cell *81*, 117–127.

Wang, S.Z., and Adler, R. (1995). Chromokinesin: a DNA-binding, kinesin-like nuclear protein. J. Cell Biol. *128*, 761–768.

Weller, M., Schulz, J.B., Wüllner, U., Löschmann, P.A., Klockgether, T., and Dichagans, J. (1997). Developmental and genetic regulation of programmed neuronal death. J. Neural Transm. Suppl. *50*, 115–123.

Yuan, J., and Yankner, B.A. (2000). Apoptosis in the nervous system. Nature *407*, 802–809.